

Multiplication of shear bands and ductility of metallic glass

F. F. Wu^{a)} and Z. F. Zhang^{b)}

Shenyang National Laboratory for Materials Science, Institute of Metal Research, The Chinese Academy of Sciences, 72 Wenhua Road, Shenyang 110016, China

F. Jiang and J. Sun

State Key Laboratory for Mechanical Behavior of Materials, Xi'an Jiaotong University, Xi'an 710049, China

J. Shen

School of Materials Science and Engineering, Harbin Institute of Technology, Harbin 150001, China

S. X. Mao

Department of Mechanical Engineering, University of Pittsburgh, 648 Benedum Hall, Pittsburgh, Pennsylvania 15261

(Received 7 March 2007; accepted 17 April 2007; published online 9 May 2007)

The authors find that metallic glass can be controlled to create regularly arrayed fine multiple shear bands under small punch test, indicating that metallic glass essentially has a good plastic deformation ability and thus high ductility under suitable loading condition. The current findings imply that the initiation and propagation of shear bands in metallic glass strongly depends on the stress state and the small punch test can also be regarded as an effective method to characterize the shear deformation ability and distinguish ductile-brittle transition of different metallic glasses.

© 2007 American Institute of Physics. [DOI: 10.1063/1.2738366]

As is well known, ductile crystalline metallic materials can undergo large plastic deformation because of their easy slip deformation feature and good strain hardening ability. However, due to the lack of strain hardening in metallic glass, the shear bands often propagate fast so that metallic glasses are very easy to fail catastrophically. Therefore, it is often considered that metallic glasses cannot accommodate large macroscopic plastic deformation although individual shear band has a shear strain as high as $10^2\% - 10^3\%$.¹ This problem makes metallic glasses difficult to be extensively applied in engineering fields. To circumvent this problem, several approaches have been tried in the past decades to create more homogeneous shear bands in various metallic glasses. The most common method is to introduce ductile second phases to inhibit the fast propagation of shear bands,^{2,3} leading to the formation of multiple shear bands and an enhanced plasticity. Over recent years, some monolithic metallic glasses were found to exhibit great compressive plasticity, which is attributed to the high Poisson ratio or low G/B (G and B are the elastic shear and volume moduli, respectively).^{4,5} Recently it is found that metallic glasses can also display increased plasticity in bending and compression through controlling the surface residual stress induced by shot peening.⁶ Besides, it is noted that the geometry of metallic glass specimens also plays an important role in the formation of shear bands and the plastic deformation capability.⁷ As the aspect ratio of the specimen is lowered down to less than 1, multiple shear bands are easy to form and the metallic glass shows a large plasticity.⁸ Alternatively, by applying multiaxial compression,^{9,10} in contrast to the catastrophic shear fracture in uniaxial compression, metallic glass exhibits large inelastic deformation with plastic strain

of more than 10% under confinement,¹⁰ demonstrating the nature of ductile deformation under constrained conditions. In the present work, we apply a multiaxial loading method to create multiple shear bands in metallic glass. The produced shear bands distribute homogeneously with regular pattern, which was seldom found in metallic glasses before.

The alloy ingot with nominal composition $\text{Cu}_{47.5}\text{Zr}_{47.5}\text{Al}_5$ (at. %) was prepared by arc melting mixtures of ultrasonically cleansed Zr (crystal bar), Cu, and Al pieces with purity of 99.9 at. % or better. The final ingots have a rectangle shape with a dimension of $30 \times 30 \times 2 \text{ mm}^3$. The microstructures and the phases of the prepared ingot were characterized by using a Leo Super 55 scanning electron microscope (SEM), as well as by using a Rigaku diffractometer with $\text{Cu } K\alpha$ radiation. The final ingot shows only broad diffraction maxima and no peaks of crystalline phases can be seen, revealing the amorphous structure of the sample. The mechanical behavior of the $\text{Cu}_{47.5}\text{Zr}_{47.5}\text{Al}_5$ bulk metallic glass (BMG) was directly measured using the small punch testing technique.¹¹ The dimensions of the specimens are $500 \mu\text{m}$ in thickness and 10 mm in diameter. The specimens were sandwiched between the upper and lower dies, as shown in Fig. 1(a). The small punch tests were performed with a MTS810 testing machine at room temperature. All the tests were conducted using a constant cross-head rate of about 0.075 mm/min. After punch tests, all the specimens were observed by LEO Super 35 SEM and Olympus LEXT OLS3000 laser confocal scanning microscope (LCSM) to reveal the deformation and fracture features and quantitatively measure the height of the shear steps.

The $\text{Cu}_{47.5}\text{Zr}_{47.5}\text{Al}_5$ BMG specimens were subjected to the small punch test, as schematically illustrated in Fig. 1(a). Figure 1(b) shows the load-deflection curve of the BMG specimens after the small punch test. The curves can be generally divided into three regions: elastic region, plastic region, and fracture region,¹² as respectively marked with A,

^{a)}Electronic mail: ffwu@imr.ac.cn

^{b)}Author to whom correspondence should be addressed; electronic mail: zhzhzhang@imr.ac.cn

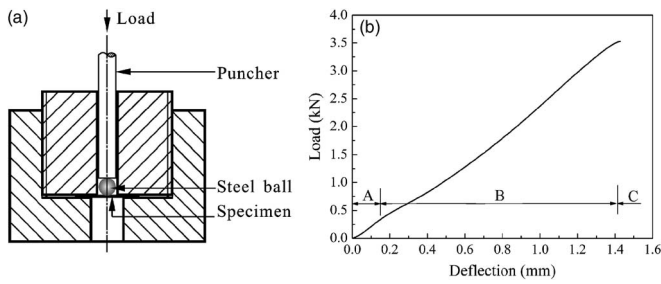


FIG. 1. Small punch test clips and load-deflection curves. (a) The schematic illustration of small punch test: the disc metallic glass specimen was clipped in the upper and lower dies; and (b) the load-deflection curve achieved by the small punch test for a disc metallic glass specimen: the marked A, B, and C represent the elastic, plastic, and fracture regions, respectively.

B, and C in Fig. 1(b). In the elastic region, the initial stiffness is 2.3 kN mm^{-1} on average, which is decided by the elastic modulus, the thickness of the specimen, and the geometry of the dies. In the plastic region, by comparing the load-deflection curve with the plastic bending model and plastic membrane stretching model based on the perfect rigid plastic model of Onat and Haythornthwaite,¹³ at first, the experimental result is in good agreement with the plastic bending solution,¹² and then falls between the plastic bending and membrane stretching solution. When the load reaches the peak value, the specimens lost their load carrying capacity immediately and fall into failure abruptly.

Figure 2 presents the deformation features of the BMG specimen after the small punch test. There are two kinds of shear bands, i.e., radial shear bands and circumferential shear bands, which look like a cobweb, as shown in Figs. 2(a) and 2(b). According to the stress distribution of the punched specimens, there exist two kinds of maximum normal stresses, i.e., radial normal stress σ_r and circumferential normal stress σ_θ , exerting on the specimens, as shown in Fig. 2(c). Due to the symmetry of the specimen, both σ_r and σ_θ are primary stresses. At any plane the circumferential normal stress σ_θ can be resolved into a maximum shear stress and

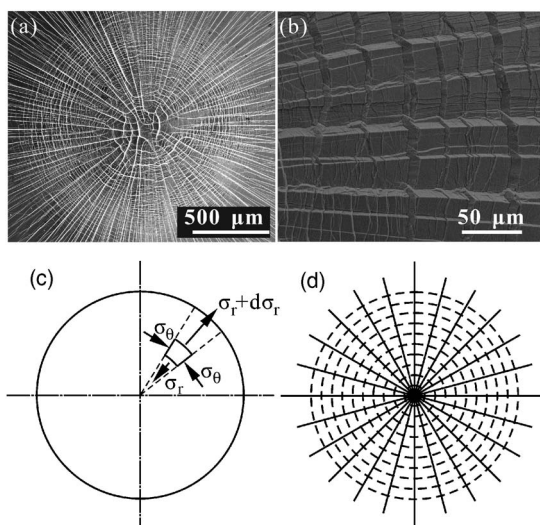


FIG. 2. Morphology of shear bands on the lower surface of the metallic glass specimens after small punch test. [(a) and (b)] SEM images of shear bands on the lower surface of the specimens after test; (c) illustration for the stress distribution state; and (d) illustration for the corresponding shear bands morphology of the lower surface of the specimen subjected to small punch.

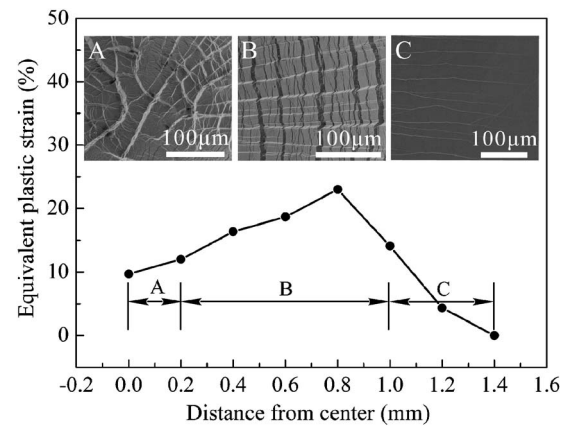


FIG. 3. Equivalent plastic strain showed that deformation degree changes obviously with the radial position away from the punch center: in region A, the shear bands are of disorder; in region B, dense, regular radial, and circumferential shear bands are formed; and in region C, circumferential shear bands vanish and only radial shear bands can be seen.

normal stress. When the maximum shear stress increases to the critical shear strength of the BMG material, shear bands will firstly initiate and propagate along the radial direction if considering the Tresca criterion [Fig. 2(d)]. Similarly, the radial normal stress σ_r can also be resolved into a maximum shear stress, which leads to the formation of circumferential shear bands along the circles around the center of the punched area [Fig. 2(d)]. Finally, due to the coexistence of σ_θ and σ_r at any plane, the radial and circumferential shear bands form and interact with each other, leading to an interlaced multiplication. With further propagation of those interacting shear bands, more shear bands will emerge to relax the accumulated stress. Profuse multiple shear bands in both radial and circumferential directions form the fine and regular shear band patterns, as shown in Fig. 2(a), indicating a good plastic deformation ability.

Based on the experimental observations on the fracture of the punched specimen that occurred after membrane stretching, fracture stretching can be calculated by using the membrane theory proposed by Chakrabarty.¹⁴ Since the radial and circumferential strains are the same, the equivalent plastic strains along the radius of the punched specimen can be expressed by

$$\varepsilon_q = \ln(t_0/t), \quad (1)$$

where t_0 and t are the thicknesses of the specimen before and after punch test, respectively.¹² By measuring the thickness t of the punched specimen at different positions, the equivalent plastic strain along the radius of the specimen can be calculated and is given in Fig. 3. It shows that the specimen underwent severe plastic deformation and the deformation degree changed obviously with the radial position away from the punch center. In the center, the equivalent plastic strain is about 9%, and the shear bands in region A are of disorder, as shown in Fig. 3. With increasing the distance away from the center, the equivalent plastic strain increases, forming a high density of shear bands, as shown in Fig. 3 in detail. The regular radial and circumferential shear bands form a cross-weaved structure. A peak equivalent plastic strain of 23% is achieved at the position 0.8 mm away from the center, which is higher than the plastic strain of 16% measured by Das *et al.* through uniaxial compressive test of the $\text{Cu}_{47.5}\text{Zr}_{47.5}\text{Al}_5$ BMG sample.⁵ The density of shear bands is the highest in

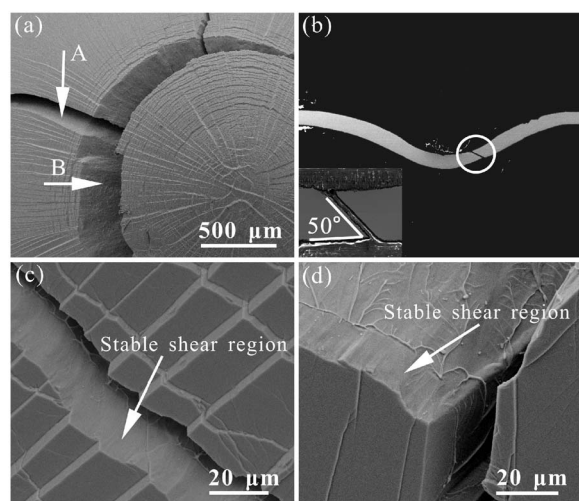


FIG. 4. Fracture features of the specimen after small punch test: (a) radial and circumferential cracks (indicated by arrows A and B); (b) the cross section of the failed specimens shows the fracture angle; and [(c) and (d)] the magnified images of the circumferential cracks show the stable shear regions.

region B (marked in Fig. 3) and the observations under LCSM show that the surface steps caused by shear offset are some $5\ \mu\text{m}$. Then the equivalent plastic strain decreases sharply with further increasing the radial distance. At a certain distance (region C in Fig. 3), the circumferential stress plays a dominating role in the formation of shear bands and the radial stress has less effect on the shear bands forming. Therefore, the circumferential shear bands begin to vanish and only radial shear bands can be seen, as shown in Figs. 2(a) and 3. Meanwhile, the shear deformation degree of the radial shear bands gradually becomes weak and finally disappears, as shown in Fig. 3(c).

Figure 4 shows the fracture features of the punched specimens at a rather high magnification. The fracture basically occurred in two modes: i.e., radial fracture [arrow A in Fig. 4(a)] and circumferential fracture at the punch center [arrow B in Fig. 4(a)]. Further observations show that there are also some vein patterns on the fracture surface, which is similar to that on the uniaxial tensile fracture surface,¹ as shown in Figs. 4(c) and 4(d). Meanwhile, it is found that the circumferential fracture often takes place prior to the radial fracture, indicating that the circumferential plastic deformation compatibility is more difficult than the radial one. From Fig. 4(b), it can be seen that the shear crack often occurred at the necking location, then propagated along the 50° declined plane, neither along the plane perpendicular to the specimen thickness nor along the 45° declined plane. This is because in this region the deformation is in a combined state of membrane stretching and plastic bending,¹² as a result, forming the vein pattern similar to the tensile fracture feature.¹⁵ When the shear crack propagated to some extent, the punched specimen lost its load carrying capacity very quickly. From Fig. 4(b), it can be seen that the crack formed in the region where the largest plastic deformation took place, therefore it seems that the failure of the punched specimen is mainly controlled by the equivalent fracture strain under the current biaxial stress state. On the margin of the fracture surface, as indicated by the arrows in Figs. 4(c) and 4(d), there is a continuous $10\text{--}40\ \mu\text{m}$ plain region without veinlike pattern,

which should correspond to the initial slow initiation of shear bands. This proves that the plastic strain in an individual shear band can be very large. Given that the average width of the shear band is about $10\ \text{nm}$,¹⁶ the shear plastic strain within an individual shear band is estimated to be about $(1\text{--}4) \times 10^4\%$, which is higher than the shear plastic strain of $10^2\% \text{--} 10^3\%$ reported by Chen *et al.*¹ This indicates that the individual shear band in BMG can accommodate extremely high shear plastic strain under suitable loading condition. Besides, there is an extensive region with veinlike patterns, which corresponds to the fast propagation of shear bands and the final failure of the specimens subjected to small punch tests.

In summary, in contrast with the few primary shear bands and catastrophic failure under uniaxial compressive or tensile loading, the metallic glass displays very good deformation ability with the formation of regular multiple shear bands and high ductility when it is subjected to small punch test. The creating multiple shear bands should result from the complex biaxial stress state existing in the BMG specimen, indicating that some metallic glasses essentially has a good plastic deformation ability and thus high ductility. Due to the easy multiplication of shear bands without catastrophic failure, the small punch test can be considered as an effective method to measure the intrinsic ductility of different metallic glasses, or to distinguish their ductile-brittle transition behavior, as well as the fracture toughness similarly in intermetallics, ceramics, or biomaterials.^{17,18} To further understand the deformation and fracture behaviors of various metallic glasses under small punch loading, there are still abundant investigations to be carried out and clarified in the future.

The authors would like to thank W. Gao, H. H. Su, and G. Yao for mechanical tests and SEM observations. This work was financially supported by the National Outstanding Young Scientist Foundation for one of the authors (Z.F.Z.) under Grant No. 50625103, the National Natural Science Foundation of China (NSFC) under Grant Nos. 50401019 and 50501017 and 2004CB619300, the ‘‘Hundred of Talents Project’’ by the Chinese Academy of Sciences, and the Shenyang Center of Interfacial Materials (CIM).

¹H. Chen, Y. He, G. J. Shiflet, and S. J. Poon, *Nature (London)* **367**, 541 (1994).

²R. D. Conner, H. Choi-Yim, and W. L. Johnson, *J. Mater. Res.* **14**, 3292 (1999).

³C. C. Hays, C. P. Kim, and W. L. Johnson, *Phys. Rev. Lett.* **84**, 2901 (2000).

⁴J. Schroers and W. L. Johnson, *Phys. Rev. Lett.* **93**, 255506 (2004).

⁵J. Das, M. B. Tang, K. B. Kim, R. Theissmann, F. Baier, W. H. Wang, and J. Eckert, *Phys. Rev. Lett.* **94**, 205501 (2005).

⁶Y. Zhang, W. H. Wang, and A. L. Greer, *Nat. Mater.* **5**, 857 (2006).

⁷F. F. Wu, Z. F. Zhang, and S. X. Mao, *J. Mater. Res.* **22**, 501 (2007).

⁸Z. F. Zhang, H. Zhang, X. F. Pan, J. Das, and J. Eckert, *Philos. Mag. Lett.* **85**, 513 (2005).

⁹J. J. Lewandowski and P. Lowhaphandu, *Philos. Mag. A* **82**, 3427 (2002).

¹⁰J. Lu and G. Ravichandran, *J. Mater. Res.* **18**, 2039 (2003).

¹¹X. Mao, M. Saito, and H. Takahashi, *Scr. Metall. Mater.* **25**, 2481 (1991).

¹²X. Y. Mao, T. Shoji, and H. Takahashi, *J. Test. Eval.* **15**, 30 (1987).

¹³E. T. Onat and R. M. Haythornthwaite, *J. Appl. Mech.* **23**, 49 (1956).

¹⁴J. Chakrabarty, *Int. J. Mech. Sci.* **12**, 315 (1970).

¹⁵Z. F. Zhang, J. Eckert, and L. Schultz, *Acta Mater.* **51**, 1167 (2003).

¹⁶P. E. Donovan and W. M. Stobbs, *Acta Metall.* **29**, 1419 (1981).

¹⁷J. F. Li and R. Watanabe, *Mater. Trans., JIM* **40**, 508 (1999).

¹⁸S. X. Mao, N. A. McMinn, and N. Q. Wu, *Mater. Sci. Eng., A* **363**, 275 (2003).